

Site Specificity in Vimentin–Membrane Interactions: Intermediate Filament Subunits Associate with the Plasma Membrane via Their Head Domains

SPYROS D. GEORGATOS,* DANIEL C. WEAVER,† and VINCENT T. MARCHESI

Department of Pathology Yale University School of Medicine, New Haven, Connecticut 06510.

*Dr. Georgatos' present address is Laboratory of Cell Biology, The Rockefeller University,

New York City, New York. †Dr. Weaver's present address is University of Cincinnati Medical Center, Department of Pathology M. L. 529, Cincinnati, Ohio 45267.

ABSTRACT Fragments of vimentin, generated by chemical or enzymatic cleavages, were analyzed for their capacity to bind to human inverted erythrocyte membrane vesicles. Only peptides comprising the amino-terminal head domain of vimentin molecules were competent in associating with the membranes. In vitro studies also demonstrated that isolated ankyrin (the major vimentin acceptor site on the membrane) binds to an oligomeric species of vimentin and prevents the formation of characteristic 10-nm filaments. These data, taken together with the observation that the NH₂-terminal end of vimentin is implicated in the polymerization process (Traub, P., and C. Vorgias, *J. Cell Sci.*, 1983, 63:43–67), imply that intermediate filaments may contact the membrane in an end-on fashion, using the exposed head domains of their terminal subunits.

Vimentin binds to inverted human erythrocyte membrane vesicles, or inside-out membrane vesicles (IOVs)¹ through a high-affinity association with ankyrin, one of the major components of the membrane skeleton (1). The characteristics of the association suggest that ankyrin may serve as an attachment site for intermediate filaments through an end-on association mechanism. Vimentin possesses a tripartite molecular substructure composed of a head piece, a helical middle domain, and a tail region (2, 3). It undergoes polymerization via lateral associations of individual monomers followed by an elongation of short protofilaments, to form extended 10-nm filaments (4). The amino-terminal head domains are implicated in this latter step (5).

The studies described below show that vimentin molecules bind to membranes through their amino-terminal domains, and, as it could be expected, the binding of ankyrin to vimentin oligomers inhibits the formation of higher polymers in vitro.

¹ Abbreviations used in this paper: IOVs, inside-out membrane vesicles; NTCB, 2-nitro-5-thiocyanobenzoic acid; PMSF, phenylmethylsulfonyl fluoride.

MATERIALS AND METHODS

Chemicals: α -Chymotrypsin was purchased from Worthington Biochemical Corp., (Freehold, NJ) trypsin from Miles Laboratories, Inc., (Elkhart, IN). 2-Nitro-5-thiocyanobenzoic acid (NTCB) was synthesized according to the method of Degani and Patchornic (6).

Purification of Vimentin: In a typical experiment, 50 calf lenses (44–50 g) were homogenized in phosphate-buffered saline (PBS) containing 2 mM MgCl₂, 5 mM 2-mercaptoethanol and 1 mM phenylmethylsulfonyl fluoride (PMSF) (pH 7.4) at 4°C. After centrifugation in a JA14 Beckman rotor at 14,000 rpm for 40 min, the pellet was extracted for 15 min with 0.6 M KCl, 50 mM Tris-HCl, 2 mM MgCl₂, 5 mM 2-mercaptoethanol, 1 mM PMSF, 1 mM NaN₃, and 0.5% Triton X-100 (pH 7.4) on ice; it was then Dounce-homogenized (12 strokes) and spun for 45 min. This procedure was repeated three times. The final pellet was washed with 150 mM KCl, 5 mM Tris-HCl, 5 mM 2-mercaptoethanol, 1 mM PMSF, and 1 mM NaN₃ (pH 7.4), and then extracted with 7 M urea, 2 mM Tris-HCl, 10 mM EDTA, 5 mM 2-mercaptoethanol, 1 mM PMSF (pH 7.4) (3 h at 23°C or 8 h at 4°C with 6 M urea). The extract was high-speed centrifuged (100,000 g for 30 min) after dilution (1:1) with double-distilled water, and the supernate was collected. Urea was removed by dialysis against 2 mM Tris-HCl, 1 mM EDTA, 5 mM 2-mercaptoethanol, 0.2 mM PMSF (pH 7.4), and vimentin was precipitated with ammonium sulfate at 23°C saturation. The precipitate was resuspended in 6 M urea, 5 mM Tris-HCl, 1 mM EDTA, 2 mM 2-mercaptoethanol, 0.1 mM PMSF (pH 7.6), and dialyzed against the same buffer. After adjustment of the protein concentration to ~1 mg/ml, this material was combined batchwise with DEAE-cellulose (DE52) equilibrated in the same buffer, shaken for 30 min at 4°C, and

extensively washed with 2 liters of the low-salt buffer. The resin was poured into a column, washed with another 2 bed volumes of buffer, and finally eluted with a 0–300-mM NaCl gradient. Vimentin-containing fractions were identified by SDS PAGE, pooled, dialyzed for 2–3 d against 3 mM NaPO₄, 0.1 mM EDTA, 2 mM 2-mercaptoethanol, and 0.1 mM PMSF (pH 7.4), and the protein concentration was adjusted to 0.1–0.4 mg/ml. The preparation was kept in 1-ml aliquots at 0°C and remained stable over the course of at least 1 mo. Upon addition of salt (to isotonic) characteristic 10-nm filaments were formed *in vitro*. (The purification and radiolabeling of vimentin are shown in Fig. 8.)

Purification of Ankyrin: Ankyrin was isolated from human erythrocyte ghosts as previously described (7).

Chymotryptic Cleavages of Vimentin: Digestion of purified vimentin was performed at 23°C with α -chymotrypsin at an enzyme to substrate ratio of 1:250 for 1, 15, and 30 min or at 4°C for 2 min. Digestion was stopped by the addition of PMSF to 1.3 mM and cooling on ice. Digests remained stable for at least 1 wk.

Chemical Cleavage of Vimentin: Purified vimentin (200 μ g/ml) was made 6 M in urea by the addition of solid urea, and then dialyzed against 6 M urea, 40 mM Tris-HCl, 1 mM EDTA, and 0.1 mM PMSF (pH 8.0). NTCB was then added at 2 mM and the preparation was incubated for 40 min at room temperature. After that, the pH was raised to 9 by the addition of Tris base and the reaction mixture was incubated at 37°C for 4 and 8 h. The reaction was stopped by the addition of 2-mercaptoethanol to 10 mM and samples were subsequently dialyzed extensively against 3 mM NaPO₄, 0.1 mM PMSF, 2 mM 2-mercaptoethanol (pH 7.4).

Radiolabeling Procedures: Purified vimentin (at 90–100 μ g/ml), or NTCB-cleaved vimentin (220 μ g/ml) were dialyzed against 50 mM NaPO₄ (pH 8.1) and then reacted with low-specific activity (500 Ci/mmol) Bolton-Hunter reagent-¹²⁵I. Reaction was allowed to proceed for 30 min at 0°C after which the proteins were extensively dialyzed against 3 mM NaPO₄, 0.1 mM EDTA, 1 mM PMSF (pH 7.4). Specific activities varied between 50 and 70,000 cpm/ μ g. Protein-bound radioactivity was estimated to 99.1% after precipitation with trichloroacetic acid (10%) at 0°C, in the presence of 3% bovine serum albumin (BSA) (carrier protein).

Immunoprecipitation: ¹²⁵I-Vimentin (33,000 cpm/ μ g) was incubated with 17 μ g/ml of isolated ankyrin (30 min in 20 mM KCl, 5 mM Tris, 0.5 mM PMSF [pH 7.4] and 30 min at 100 mM KCl, 10 mM Tris, 0.1 mM PMSF [pH 7.4]) at 23°C in a final volume of 100 μ l and in the presence of 0.1 mg/ml BSA. After that, 3 μ l of anti-ankyrin antiserum or nonimmune serum were added, and the proteins were incubated for an additional 30 min at 23°C. 20 μ l of a *Staphylococcus aureus* suspension were then pipetted and, after 15 min, the samples were centrifuged (5 min in a minifuge). Pellets were washed five times with 100 mM KCl, 10 mM Tris, 0.1 mM PMSF (pH 7.4) containing 0.06% Triton X-100. The combined supernates and the pellets were then counted in a gamma counter.

Sedimentation Assays: ¹²⁵I-Vimentin (10,000 cpm/ μ g) and purified ankyrin were prespun at 25 psi for 30 min in an airfuge. Then, increasing amounts of ankyrin were incubated for 30 min with vimentin in 20 mM KCl, 5 mM Tris, 0.1 mM PMSF (pH 7.4) at 23°C (or alternatively in PBS/10). After this incubation, the salt was adjusted to 100 mM KCl, 10 mM Tris, 2 mM 2-mercaptoethanol (pH 7.4), and an additional 60-min incubation ensued. In some cases, the two proteins were simply dialyzed together against low salt (overnight at 4°C) and then against PBS (3 h at 23°C). The samples were placed in airfuge tubes over a 100- μ l cushion of 10% sucrose in the assay buffer and spun for 30–35 min at 25 psi. The tubes were next frozen in liquid N₂, dissected with a razor blade (supernate/pellet) and counted as above.

Negative Staining: Vimentin alone (300 μ g/ml) or vimentin mixed with ankyrin were prespun and incubated as described above for the sedimentation assays. 30 μ l of each sample were then applied to glow-discharged electron microscope grids for 1 min at room temperature. Excess liquid was removed by capillary action and phosphotungstic acid (3% phosphotungstic acid prepared fresh) was added for 2 min after which 1% uranyl acetate was applied for 1 additional min. Grids were visualized in a Phillips 300 electron microscope.

Electrophoresis: One- and two-dimensional electrophoresis was performed as previously described (8, 9).

Protein concentrations were measured by the method of Lowry (10) using BSA as a standard.

RESULTS

Vimentin Binds to IOVs through its Head Domain

Treatment of vimentin with NTCB is known to cleave the polypeptide chain at a single cysteine residue, 137 amino acids from the COOH-terminal, and to separate the molecule

into two segments. One (C-I) contains the amino-terminal head domain and part of the middle domain and the second (C-II) is composed of the tail region and the remainder of the middle segment (2, 3). When the two NTCB fragments of vimentin are incubated with IOVs under physiological conditions, only one, the C-I fragment binds selectively to the surfaces of the IOVs (Fig. 1). The specificity of the binding of this 37,000-mol-wt fragment to IOVs is demonstrated by showing that unlabeled intact vimentin molecules were able to quantitatively displace both labeled intact vimentin and the labeled C-I peptide (Fig. 2). The data shown in Fig. 2 show that unlabeled intact vimentin molecules are able to displace labeled vimentin molecules to a greater extent than the labeled C-I peptides, as would be expected from the difference in molar concentrations of the two peptides. (The molar ratio between C-I and uncleaved vimentin in this particular digest was estimated to 1.52:1). It is worth noting that some products of endogenous degradation (probably lacking the head domain and migrating between uncleaved vimentin and C-I or between C-I and CII) also partition with the supernate.

Since the C-I peptide derived from vimentin is composed of both the head domain of the molecule and part of the middle segment, further analysis was carried out using limited chymotryptic digestion. Brief incubations of intact vimentin with low concentrations of chymotrypsin at room temperature produced a series of peptides with molecular weights of 55,000, 50,000, 47,000, and 45,000. This characteristic “stair-

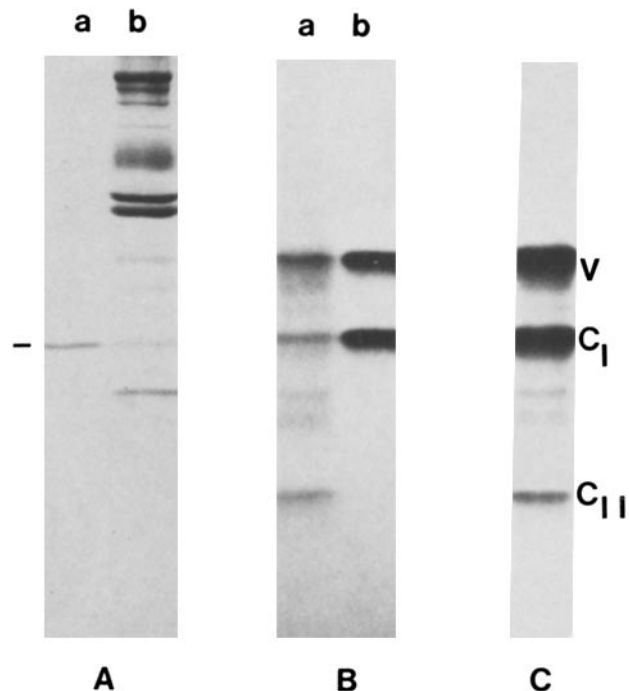


FIGURE 1 Binding of ¹²⁵I-vimentin NTCB fragments to IOVs. 55 μ g of IOVs were incubated with 2.25 μ g of ¹²⁵I-vimentin NTCB fragments in PBS at pH 7.4 and in a final volume of 110 μ l. After 90 min, the reaction mixture was centrifuged through a 150- μ l cushion of 4% isotonic-sucrose, and the supernate and pellet were analyzed by SDS PAGE. (Panel A) Coomassie Blue-stained SDS gels. Supernate (a) and pellet (b). The major band in a is the band 6 polypeptide. (Panel B) Autoradiograms of the a and b fractions of panel A. (Panel C) Autoradiogram of the NTCB digest (without IOV; 4.5 μ g). V, Uncleaved vimentin; C_I, amino-terminal NTCB fragment of vimentin; C_{II}, COOH-terminal NTCB-fragment of vimentin.

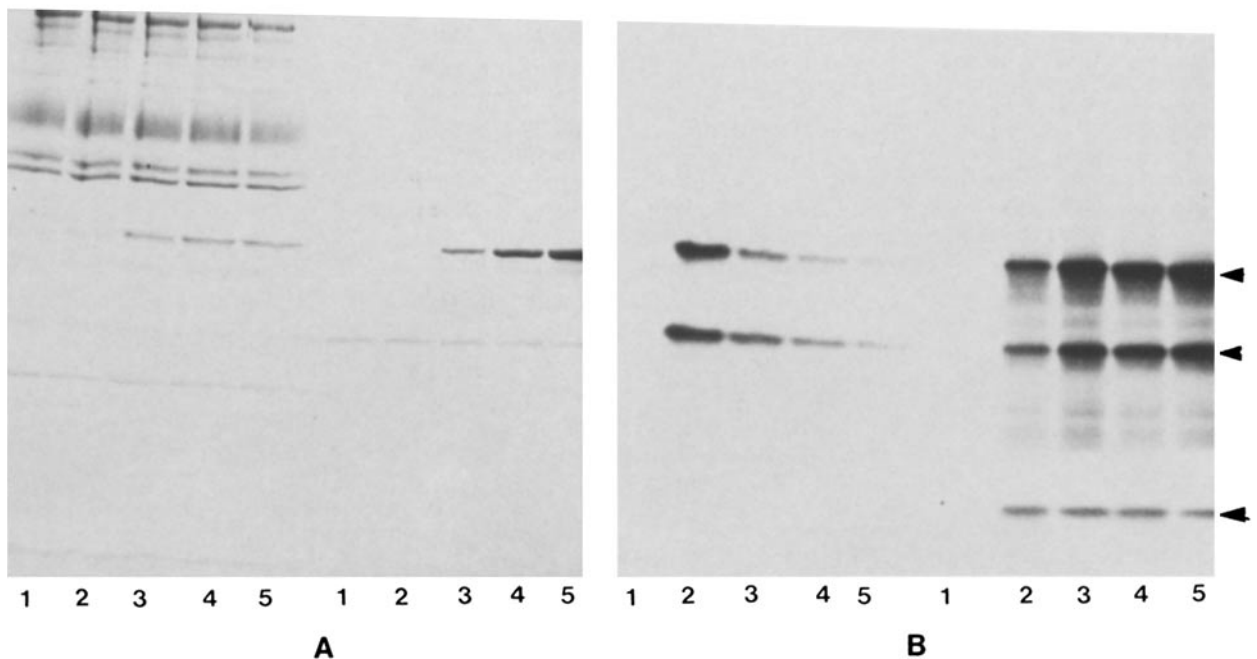


FIGURE 2 Displacement of ^{125}I -vimentin NTCB fragments bound to IOVs by unlabeled, intact vimentin. 20 μg of IOVs were incubated with a standard amount of NTCB fragments of ^{125}I -vimentin (1.1 μg) and 0 μg (2), 1.5 μg (3), 3.5 μg (4), and 5.25 μg (5) of unlabeled, intact vimentin in PBS (pH 7.4), and in a final volume of 100 μl . Sample 1 contained only IOVs. All five samples were processed as in Fig. 1. (Panel A) 1–5 (left), pellets; 1–5 (right), supernates (Coomassie-stained gel). (Panel B) Corresponding autoradiogram. Arrowheads denote (from top to bottom) the positions of intact ^{125}I -vimentin, C_I , and C_{II} .

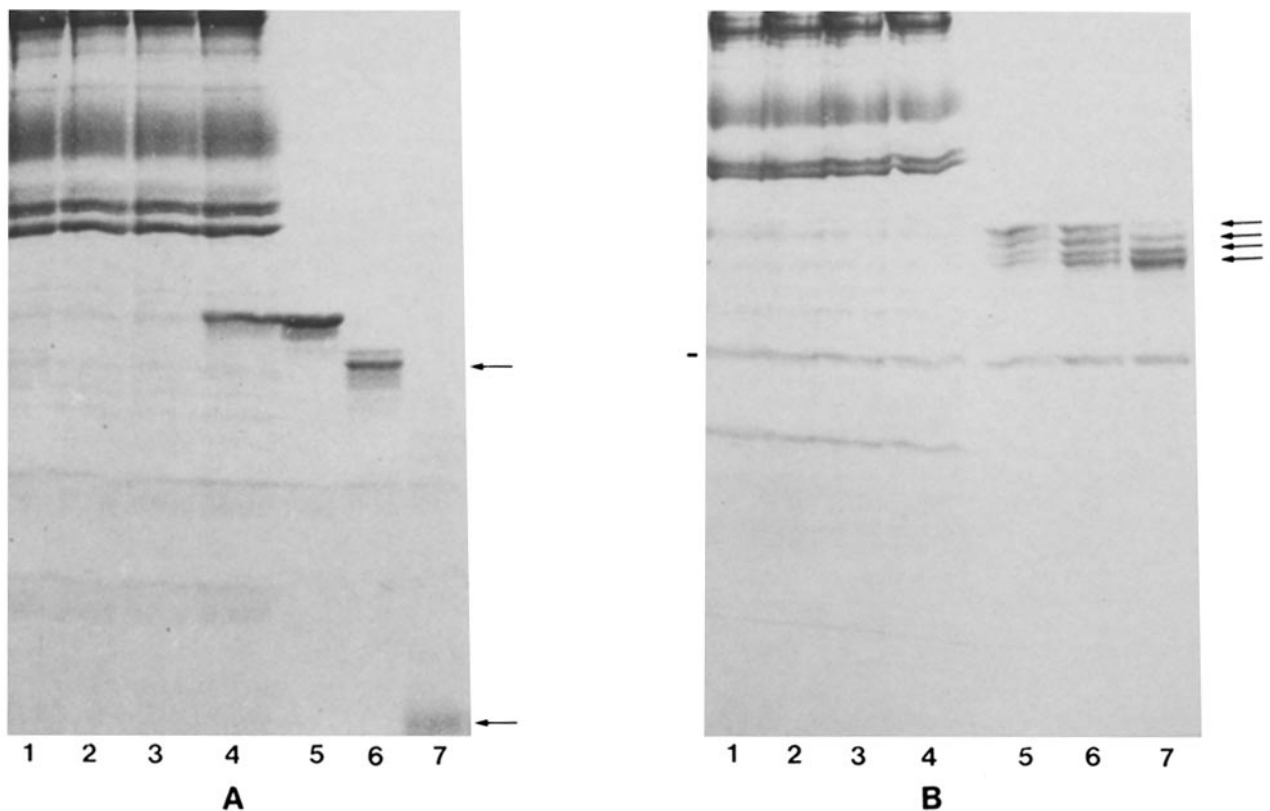


FIGURE 3 Binding of chymotryptic fragments of vimentin to IOVs. 15 μg of purified vimentin were digested at room temperature for various times with α -chymotrypsin. The reaction was stopped by the addition of PMSF to a final concentration of 1.5–2.0 mM. The digests were incubated with IOVs in PBS, 0.5 mM PMSF for 90 min at 23°C, processed as in Fig. 1, analyzed by SDS PAGE, and stained by Coomassie Blue. (Panel A) (1) 55 μg of IOVs incubated with a blank sample (no vimentin; α -chymotrypsin inhibited by PMSF); (2 and 7) 55 μg of IOVs incubated with a 30-min vimentin digest; (3 and 6) 55 μg of IOVs incubated with a 10-min digest; (4 and 5) 55 μg of IOVs incubated with 15 μg of undigested vimentin. 1–4 correspond to the membrane pellets and 5–7 to the supernates. The position of band 6 is indicated by a dash. Arrows point to the two major vimentin peptides with molecular weights of 45,000 and 22,000 (10% gel). (Panel B) (1) 20 μg of IOVs incubated with a blank sample as in A. (2 and 5) 20 μg of IOVs and 10 μg of a 30-s digest; (3 and 6) 20 μg of IOVs and a 1-min digest; (4 and 7) 20 μg of vimentin and a 2-min digest. 1–4 correspond to the membrane pellets and 5–7 to the supernates (7.5–15% gradient gel). Arrows indicate the major early fragments with apparent molecular weights of 50,000, 47,000, and 45,000. Band 6 is indicated by dash.

case pattern" of vimentin degradation results from a gradual cleavage of the vimentin molecule from the basic amino-terminal end as indicated by two-dimensional gel electrophoresis (not shown; see reference 12). More extensive degradation of vimentin produced mainly a 45,000-mol-wt peptide, analogous to desmin's 40,000-mol-wt middle piece (2, 4), then cleaved into a 22,000-mol-wt broad band analogous to the 21,000- and 18,000-mol-wt subfragments of desmin derived from the middle segment. After appropriate inhibition

of residual chymotryptic activity, the different digest fractions were analyzed for their capacity to bind to IOVs. Of the digests analyzed, no fragment showed appreciable capacity to bind to IOVs (Fig. 3), a result consistent with the idea that the active site of vimentin is contained within the protease-sensitive amino-terminal domain and not in the protease-resistant middle piece.

Ankyrin Inhibits the Assembly of Intermediate Filaments *In Vitro*

Vimentin and ankyrin form a specific complex *in vitro* that can be demonstrated by sucrose gradient centrifugation (Fig. 4). Vimentin alone at 100 $\mu\text{g}/\text{ml}$ sediments predominantly as a 6-7S species under physiologic salt and pH conditions. The addition of excess ankyrin causes a significant shift in the migrating peak (Fig. 4). Incubation of vimentin preparations with threefold excess ankyrin also causes a significant decrease in the amount of pelleted (filamentous) vimentin that is formed under these conditions.

The association between ankyrin and vimentin was also analyzed using a radioimmunoassay with anti-ankyrin antibodies. The data in Fig. 5 show that the association between vimentin and ankyrin was concentration-dependent and saturable, and corresponded roughly to a 1:1 molar stoichiometry, assuming a tetrameric organization for the vimentin oligomer (4).

Based on the results of the sedimentation experiments and the fact that the head domain of the vimentin molecule seemed to bind specifically to IOVs, we considered it likely that ankyrin might affect the capacity of vimentin molecules to polymerize into intermediate filaments by binding to the head domains of the protofilaments and thereby blocking the arginine-rich regions that are thought to be involved in the assembly process (5). This question was approached by two independent methods. Vimentin was assembled *in vitro* in the presence of increasing amounts of ankyrin, and the relative amounts of polymer that were sedimented were correlated with the ankyrin-vimentin ratio in the original reaction mixture. The data in Fig. 6 show that there is a decrease in the relative amount of vimentin species greater than 54S as a function of increasing ankyrin concentrations. In contrast, if vimentin polymers were preassembled and then incubated with increasing amounts of ankyrin for the same time intervals, such a decrease was not detected (Table I). These results are further supported by the fact that only small amounts of ankyrin co-pelleted with prepolymerized vimentin under the same conditions (not shown).

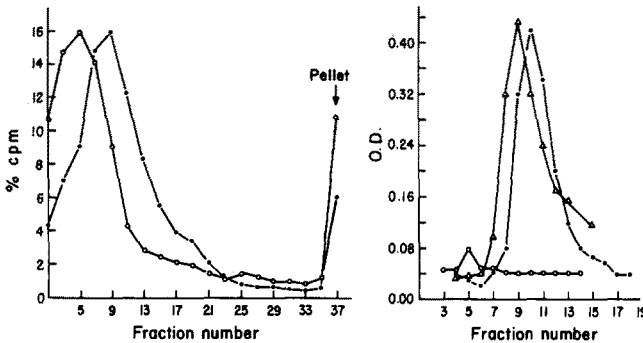


FIGURE 4 Binding of ^{125}I -vimentin to isolated ankyrin as detected by rate zonal centrifugation. ^{125}I -vimentin (100 $\mu\text{g}/\text{ml}$) was incubated with a threefold molar excess of ankyrin for 2.5 h at 4°C in PBS, 2 mM MgCl_2 , 2 mM 2-mercaptoethanol, 0.1 mM PMSF (pH 7.4), and centrifuged for 19 h in a Beckman 40 Ti rotor (40,000 rpm) at 4°C. ○, vimentin alone; ●, vimentin and ankyrin; △, ankyrin alone.

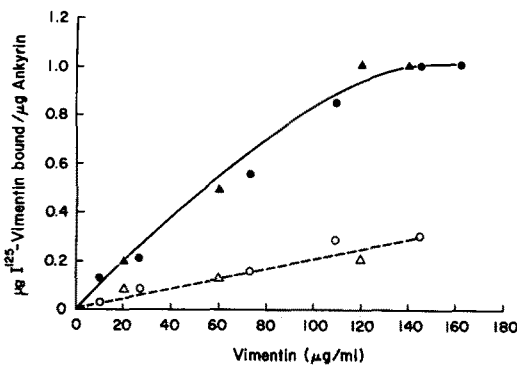


FIGURE 5 Binding of ^{125}I -vimentin to isolated ankyrin as detected by immunoprecipitation with a polyclonal anti-ankyrin antibody. ▲, ●, two separate assays with ^{125}I -vimentin, ankyrin, and anti-ankyrin (as specified in Materials and Methods) are shown. △, controls (no ankyrin added); ○, assay with normal rabbit serum instead of anti-ankyrin.

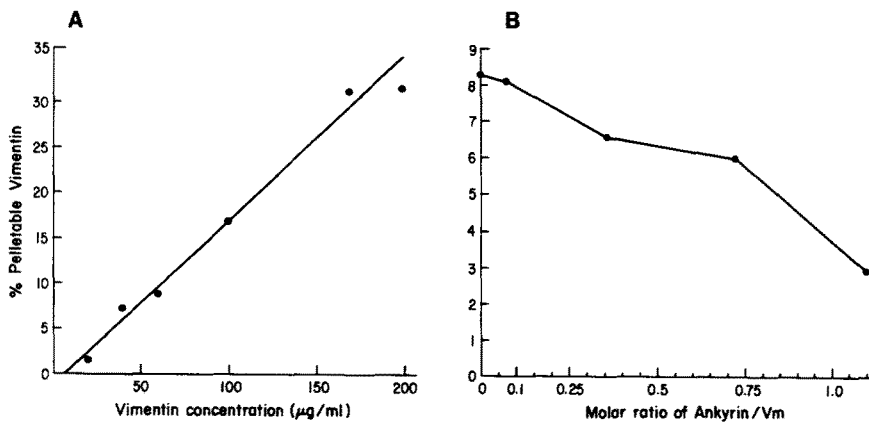


FIGURE 6 Effect of ankyrin on vimentin's polymerization as detected by sedimentation. Under the conditions of these experiments (details in Materials and Methods) only complexes greater than 54S are pelleted. (A) A standard curve indicated that the relative amounts of vimentin pelleted as a function of the protein concentration. (B) The relative amounts of vimentin pelleted after incubation with increasing amounts of ankyrin (nonassembled vimentin at 60 $\mu\text{g}/\text{ml}$). All samples were precentrifuged before the assays.

The capacity of ankyrin to inhibit the polymerization of vimentin into intermediate filaments was demonstrated most strikingly by analyzing preparations of ankyrin and vimentin by negative staining and electron microscopy (Fig. 7). Characteristic 10-nm filaments were readily demonstrated by incubation of vimentin alone (Fig. 7A), whereas no recognizable filament forms were seen when ankyrin and vimentin were incubated together before negative staining (Fig. 7, B and C). Instead, short rod-like forms were seen scattered throughout the fields. The rod-like forms had the same approximate diameter of vimentin filaments (10–11 nm); this is consistent with the idea that lateral association of protofilament units did occur, but the elongation of protofilaments was inhibited by the presence of ankyrin.

The purification and radiolabeling of vimentin are shown in Fig. 8.

DISCUSSION

The results described here and in the preceding paper (1) provide new insight into how and where intermediate filaments may attach to plasma membranes. Intermediate filaments composed of vimentin are able to bind to IOVs prepared from human erythrocytes, and they appear to do so by associating to an attachment protein, previously identified as ankyrin, which also links other components of the cytoskel-

TABLE I

Effect of Ankyrin on the Stability of Pre-assembled Vimentin Polymers under In Vitro Conditions

Concentration of vimentin $\mu\text{g/ml}$	Ankyrin/Vimentin*	Percent pelletable vimentin
60	0	8.3
60	0.05	9.4
60	0.35	9.3
100	0	20
100	0.05	18.9
100	0.35	16.4
200	0	38
200	0.35	40

Vimentin was preassembled in isotonic KCL buffer for 1 h at 23°C and then co-incubated with isolated ankyrin for additional 40 min. Samples were processed as described in Materials and Methods.

* In molar terms.

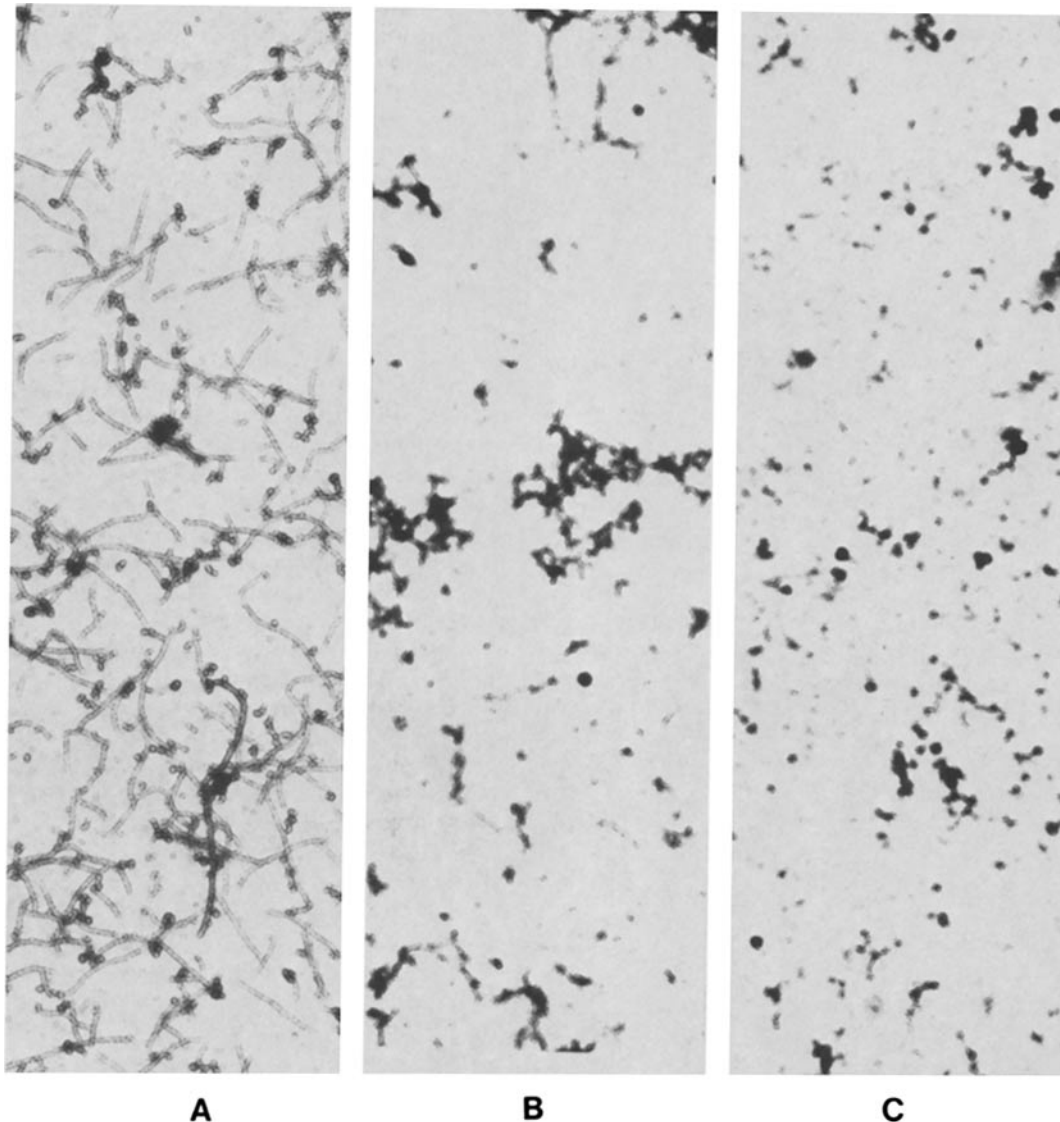


FIGURE 7 The effect of ankyrin on vimentin polymerization as detected by negative staining and electron microscopy. (A) Vimentin alone (300 $\mu\text{g/ml}$). (B) Vimentin (300 $\mu\text{g/ml}$) and ankyrin at a molar ratio of 4:1. (C) Vimentin and ankyrin at a molar ratio of 2:1. $\times 42,000$.

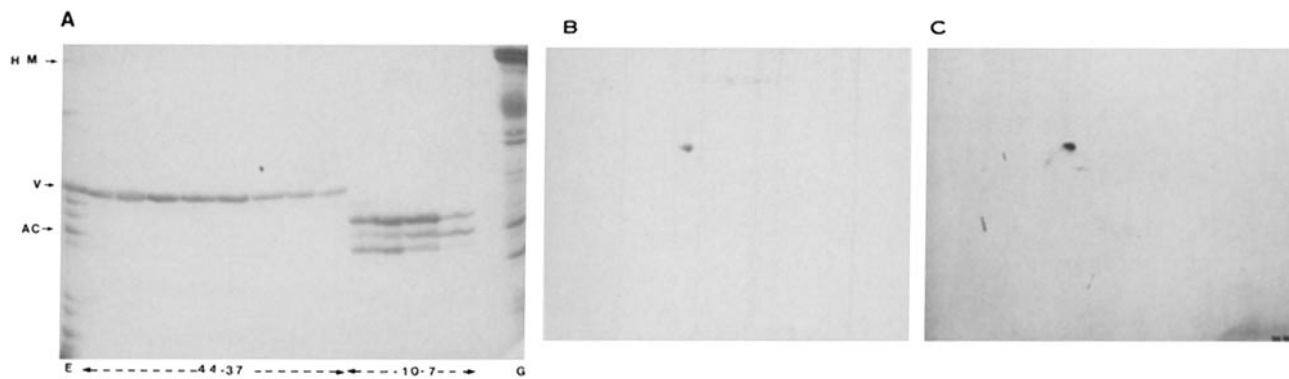


FIGURE 8 Purification and radiolabeling of vimentin. (A) SDS PAGE of various fractions recovered after ion-exchange chromatography of a urea-extract of lens cytoskeletons. E, material applied to the column; G, human erythrocyte ghosts; V, vimentin; HM, high molecular weight protein; AC, actin. (B) Two-dimensional electrophoretogram of purified vimentin. The basic side of the gel is on the right. Vimentin is focused at a pH of 5.3–5.4. (C) Autoradiogram of a similar two-dimensional gel of iodinated vimentin.

eton to the overlying lipid bilayer. The linkage between vimentin filaments and ankyrin probably occurs at the free ends of the intermediate filament polymers and involves an attachment of the “head” portion of the vimentin molecule to a binding site on ankyrin distinct from but probably close to the binding site on ankyrin for erythrocyte spectrin (Georgatos, S. D., and D. C. Weaver, manuscript in preparation).

Current models of vimentin organization postulate that the fundamental unit of intermediate filaments is a tetramer consisting of four polypeptide chains arranged in two dimeric pairs in lateral register (4). The dimers appear to be stabilized by noncovalent interactions between adjacent helical domains which form a coiled-cold (2, 4). It has been proposed that the polymerization of vimentin monomers into filamentous forms is initiated by specific binding of the arginine-rich head domains to the middle, helically coiled segments of neighboring protofilaments. This idea is supported by the following lines of evidence. Removal of the head piece of vimentin by a calcium-activated protease inhibits vimentin polymerization, and the helically coiled middle domains generated by this treatment will not polymerize into filaments *in vitro* (11, 12). The sensitivity of vimentin to protease cleavage is also sensitive to salt concentrations, consistent with the idea that once filament formation is induced, the protease-sensitive sites on the head groups are less exposed to enzymatic digestion. The portion of the head piece of vimentin that is involved in initiating polymerization seems to be rich in arginine residues, since the addition of excess amounts of free arginine prevent filament formation from intact vimentin monomers (5).

The experiments described here indicate that the head portion of the vimentin molecule also plays a critical role in the attachment of vimentin filaments to the IOVs and to the ankyrin molecule. Since isolated ankyrin molecules bind to vimentin and also inhibit the polymerization of vimentin oligomers into filamentous forms, it seems feasible to infer that the mode of attachments of vimentin filaments to the membrane represents an association similar in principle to the mode of association between vimentin protofilaments, with the head piece of the vimentin molecule playing a pivotal role.

If the mechanisms described above are also operative *in vivo*, it seems logical to hypothesize that membrane-bound vimentin does not provide nucleating centers for intermediate filament assembly, since the ankyrin-vimentin association

would be expected to inhibit filament growth at the binding ends. Thus, centers for nucleation of vimentin filaments that are attached to membranes should be located elsewhere inside cells, possibly at the nuclear envelope. If it follows that native vimentin intermediate filaments contain distinct nucleation sites and membrane attachment sites, such filaments also assume a distinct polarity within the cell. If only the ends of vimentin filaments are capable of binding to membrane-bound ankyrin sites, a limited number of such sites will be required to attach the number of vimentin filaments usually found inside cells, and this prediction agrees with earlier morphological studies in which it has been demonstrated that in certain vimentin-rich cells such as avian erythrocytes, the intermediate filaments associate at a relatively few foci along the plasma membrane rather than being diffusely distributed over the entire cell surface (13).

We thank Dr. G. Pasternack and Dr. I. Correas for useful discussions. We also thank one of the reviewers of these articles for his/her useful suggestions and the thorough reading of the manuscript.

This work is dedicated to Dr. Elias Broutzos-Bichtis.

Received for publication 27 November 1984, and in revised form 1 February 1985.

REFERENCES

- Georgatos, S. D., and V. T. Marchesi. The binding of vimentin to human erythrocyte membranes: a model system for the study of intermediate filament-membrane interactions. *J. Cell. Biol.* 100:1955–1961.
- Geisler, N., E. Kaufmann, and K. Weber. 1982. Protein chemical characterization of three structurally distinct domains along the protofilament unit of desmin 10-nm filaments. *Cell* 30:277–286.
- Quax-Jeuken, Y., W. J. Quax, and H. Bloemendal. 1983. Primary and secondary structure of hamster vimentin predicted from the nucleotide sequence. *Proc. Natl. Acad. Sci. USA* 80:3548–3552.
- Geisler, N., and K. Weber. 1982. The amino acid sequence of chicken muscle desmin provides a common structural model for intermediate filament proteins. *EMBO (Eur. Mol. Biochem. Organ.) J* 1:1649–1656.
- Traub, P., and C. Vorgias. 1983. Involvement of the N-terminal polypeptide of vimentin in the formation of intermediate filaments. *J. Cell. Sci.* 63:43–67.
- Degani, Y., and A. Patchornic. 1971. *J. Org. Chem.* 36:2727–2728.
- Weaver, D. C., and V. T. Marchesi. 1984. The structural basis of ankyrin function. *J. Biol. Chem.* 259:6165–6169.
- Laemmli, U. K. 1970. Cleavage of structural proteins during the assembly of the head of bacteriophage T4. *Nature (Lond.)* 227:680–685.
- O'Farrell, P. H. 1975. High resolution two-dimensional gel electrophoresis of proteins. *J. Biol. Chem.* 250:4007–4021.
- Lowry, O. H., N. J. Rosebrough, A. L. Farr, and R. J. Randall. 1951. Protein measurement with the Folin-phenol reagent. *J. Biol. Chem.* 143:265–275.
- Weber, K., and N. Geisler. 1982. The structural relation between intermediate filament proteins in living cells and the α -keratins of sheep wool. *EMBO (Eur. Mol. Biol. Organ.) J* 1:1155–1160.
- Nelson, J. W., and P. Traub. 1983. Proteolysis of vimentin and desmin by a Ca^{2+} -activated proteinase specific for these intermediate filament proteins. *Mol. Cell. Biol.* 3:1146–1156.
- Granger, B. L., and E. Lazarides. 1982. Structural association of synemin and vimentin in avian erythrocytes revealed by immunoelectron microscopy. *Cell* 30:263–275.